Thermochimica Acta, 233 (1994) 1–11
Elsevier Science B.V., Amsterdam
SSDI 0040-6031(93)01463-D

Mixing properties in the continuous solid solution of the system KNO_3–$NaNO_3$

H. Zamali [a], T. Jriri [b], J. Rogez [b,*], M. Jemal [a] and J.C. Mathieu [b]

[a] *Faculté des Sciences de Tunis, 1060 Tunis (Tunisia)*
[b] *Centre de Thermodynamique et de Microcalorimétrie-CNRS, 26, rue du 141ème R.I.A., 13003 Marseille (France)*

(Received 18 May 1993; accepted 6 June 1993)

Abstract

A previous reinvestigation of the binary phase diagram KNO_3–$NaNO_3$ has confirmed the existence of a continuous subsolidus solid solution. The mixing enthalpy in this solid phase, determined by solution calorimetry at 474 K, is presented. A positive and asymmetric deviation from ideality is observed. The results are well fitted by the Van Laar model.

INTRODUCTION

For several years our thermodynamic studies have focused on complex oxide systems containing alkali metals. In the presence of such elements, the strong interaction of the oxygen towards a metalloid element gives particular compounds such as borates, silicates, phosphates, carbonates, etc. The ionic binding between the metallic cation and the complex anion, which can be in a polymerised form, generally varies continuously in the sequence Li–Cs. A different stabilisation of the liquid and solid phases is then induced. The phase diagram and the thermodynamic properties represent the same general physicochemical phenomenon, i.e. the relative stability of the phases in the composition and temperture ranges. These two kinds of data are obtained by various techniques, for example differential thermal analysis or X-ray diffraction for the phase diagrams and calorimetry, partial vapour pressure or concentration cell e.m.f. measurements for the thermodynamic properties. All these data are then fitted together by means of some calculation programme in order to give a unique physicochemical picture of the systems.

Our aim is to carry out such a thermodynamic study of the binary and ternary nitrate systems $NaNO_3$–KNO_3–$CsNO_3$ which present various physicochemical particularities. (i) All these pure compounds show a

* Corresponding author.

structural phase transition in the solid state. (ii) Binary or ternary compounds have never been observed. (iii) As has been shown in a recent redetermintion of the binary phase diagram by differential thermal analysis [1–3], the great stability of the liquids induces deep depressions on the liquidus lines. The $NaNO_3$–$CsNO_3$ and KNO_3–$CsNO_3$ systems present a deep eutectic. In the $NaNO_3$–KNO_3 system the presence of a continuous subsolidus solution induces a similar azeotrope with minimum behaviour. Consequently, a ternary deep eutectic has also been observed [4]. (iv) The ternary solid state is characterised by four solid solutions, one of which is the extent in the ternary system of the continuous subsolidus solution of the binary system $NaNO_3$–KNO_3.

Thermodynamic data are available for the binary liquids [5–13]. The discrepancy of the data relative to the pure compounds (and in particular for $NaNO_3$) may induce great differences in the results of the computed phase diagrams [14–16]. A critical study of these data has been undertaken and also some redeterminations by differential scanning calorimetry have been carried out [3]. The aim of this study is to obtain the enthalpy of formation of the solid solution $(K_x, Na_{1-x})NO_3$ relative to the pure components KNO_3 and $NaNO_3$ in the same structural state. This structure named β, is of the rhomboedral type. In the KNO_3 rich domain the subsolidus solution is stable in a large temperature range. For example, the pure potassium nitrate β structure is observed between 401 K and 611 K. The stability temperature range decreases with x. At $x = 0.6$ it is still 60 K. In the $NaNO_3$ rich range, the stability domain becomes still smaller; for instance at $x = 0.2$ the temperature range is 15 K. For pure $NaNO_3$ the β structure lies between 549 K and 579 K.

EXPERIMENTAL SECTION

Measurement method

The mixing enthalpies in the continuous solid solution $(K_x, Na_{1-x})NO_3$ are determined by solution calorimetry. For dissolution of solid phases, the molten salts have more rarely been used as solvents than molten metals or molten oxides. More often the aqueous solvents have been chosen on obvious grounds of experimental convenience. In the present case the solid solution is unstable at ambient temperature so the choice of a molten salt becomes almost evident. The ternary eutectic in the system $CsNO_3$–KNO_3–$NaNO_3$ ($T_f = 413$ K) was finally selected for the following reasons: (i) The solid solution and the ternary liquid are stable in a common temperature range. (ii) The dissolution energies have the same magnitude than the expected mixing enthalpies so, the measurement unaccuracies are not excessive toward the expected mixing data. It is not the case when the chemical natures of the solute and of the solvent are very different, for

instance an oxide compound dissolved in an aqueous acidic solvent. (iii) The partial dissolution enthalpies will be further directly used in the thermodynamic study of the ternary liquid.

The dissolution temperature has been chosen as 474 K. It stays about 15 K below the solidus minimum at $x = 0.5$ in the KNO_3–$NaNO_3$ system.

In practice, inside an isothermal calorimeter and for each expected composition of the solid solution $(K_x,Na_{1-x})NO_3$ $(0 < x < 1)$, small amounts of the sample are successively dissolved in the same bath. The dissolution reaction for one mole of the liquid in the final state is

$$y(K_x,Na_{1-x})NO_3 + (1-y)S = ((K_x,Na_{1-x})NO_3)_y, S_{1-y} \quad (1)$$

Therefore, the partial dissolution enthalphy in the solvent is measured at various very low concentrations y of the solute in the bath. By extrapolation to the $y = 0$ concentration, the partial dissolution enthalpy at infinite dilution $\Delta_s H^{\infty}_{(K_x,Na_{1-x})NO_3}$ is determined. For pure sodium nitrate $(x = 0)$ and pure potassium nitrate $(x = 1)$ which constitute the reference states the equation becomes

$$yNaNO_3 + (1-y)S = (NaNO_3)_y, S_{1-y} \quad (2)$$

$$yKNO_3 + (1-y)S = (KNO_3)_y, S_{1-y} \quad (3)$$

The mixing enthalpy will then be given by

$$\Delta_m H(x) = x\Delta_s H^{\infty}_{KNO_3} + (1-x)\Delta_s H^{\infty}_{NaNO_3} - \Delta_s H^{\infty}_{(K_x,Na_{1-x})NO_3}$$

corresponding to the formation of the solid solution as

$$xKNO_3 + (1-x)NaNO_3 = (K_x,Na_{1-x})NO_3$$

Working at the infinite dilution in the solvent $(y = 0)$ imposes a set of measurements for each solid solution composition but does not present the drawbacks of working at a different value of y, which are as follows:

(i) The presently used thermodynamic cycle can of course be written at each concentration y in the bath. To realise the same value of y in the three successive reactions is not very simple in practice.

(ii) Above all, such a development at a non-zero concentration imposes the condition that the enthalpy of the residual reaction, being a resultant of the second members of eqns. (1), (2) and (3) after thermodynamic cycling, must remain zero. This reaction can be written as

$$x(KNO_3)_y,S_{1-y} + (1-x)(NaNO_3)_y,S_{1-y} = (K_x,Na_{1-x}NO_3)_y,S_{1-y} \quad (4)$$

In other words no interaction between the solute species (the cations Na^+ and K^+) must occur in the solvent S. This condition is generally realised, at

best, at infinite dilution. In this particular case, in order to confirm this fact, the dissolution enthalpies at infinite dilution of $NaNO_3$ (respectively KNO_3) in the pure solvent and in the solvent containing KNO_3 (respectively $NaNO_3$) have been compared. Within the error margin both results are identical, so the enthalpy of the reaction (4) is really zero.

Change of the reference state

At the chosen dissolution temperature T_d the solid solution β is stable only in the composition range $0.38 < x < 1$. For lower potassium nitrate concentrations this structure is stable at higher temperatures, so the partial solution enthalpy which is measured for the pure sodium nitrate for this compound is relative to the α low temperature phase. A correction is then applied to this data by removing the enthalpy of transition $\Delta_{tr}H_{\alpha-\beta}$ of the sodium nitrate at 474 K which is calculated by

$$\Delta_{tr}H(T_c) = \Delta_{tr}H(T_r) + \int_{T_r}^{T_d} (C_{p,\beta}(T) - C_{p,\alpha}(T))\,dt \quad (5)$$

where $\Delta_{tr}H(T_r)$ is the transition enthalpy at the transition temperature T_r and $C_{p,\alpha}$ and $C_{p,\beta}$ are the heat capacities of the low and high temperature phases, respectively. This correction is relatively large with respect to the expected mixing enthalpies, so it must be carefully estimated. For this reason, the enthalpy of transition and the heat capacities have been recently redetermined at the CTM–CNRS by differential scanning calorimetry giving $\Delta_{tr}H(474\,K) = 3369\,J\,mol^{-1}$ [3].

Experimental device and procedure

The various reactions described above are brought into effect inside the laboratory cell of a high temperature Tian–Calvet twin calorimeter, the experimental design of which has already been largely described in the literature [17, 18]. The cylindrical reaction cell is enclosed in a fluxmeter consisting of PtRh13%–Pt thermocouples. In the same manner a test cell is enclosed in an another fluxmeter; the thermal and electric characteristics of which are as identical as possible to those of the previous sensor. Both are connected in opposition in order to decrease the upsetting effects due to eventual thermal perturbations of the surroundings on the signal. The temperature of the outer walls of these thermopiles is kept at a constant value by means of a large alumina block; the thermal inertia of which is great. An electronic controller linked to a furnace permits the temperature of this calorimetric block to remain constant. It then constitutes the thermostat. The temperature of the reaction cell is measured at ±1 K by means of a PtRh10%–Pt thermocouple inserted in the alumina block between the two thermopiles. During all the experiments it is kept at

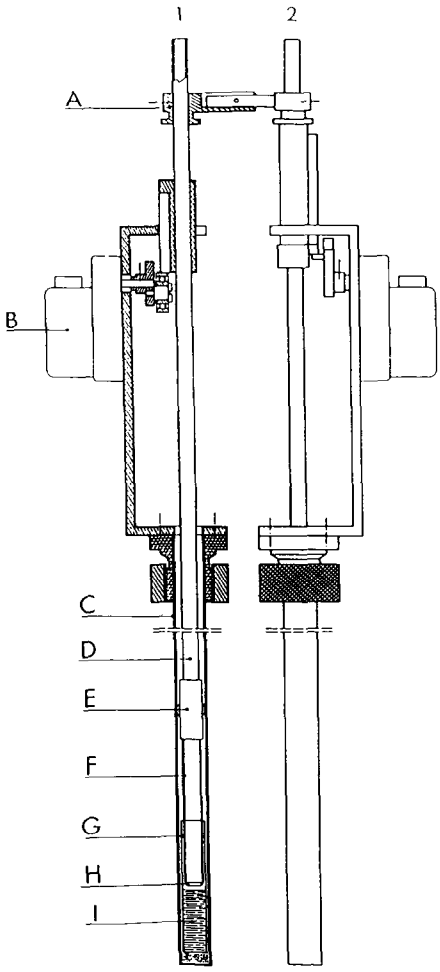

Fig. 1. Calorimetric setup: A, metallic junction pieces; B, electric motors which permit the translatory motion and if necessary the stirring of the alumina tubes D; C, quartz tube; E, alumina cement joining the alumina tube and the platinum rods F which support the plate H, (before dissolution the sample is placed on the plate); G, and platinum crucible containing the solvent I.

474 K. The thermal effect occuring during the reaction is recorded on an analogue plotter.

In Fig. 1 the presently used calorimetric equipment which has been built at CTM–CNRS is drawn. Two platinum crucibles G are introduced into the bottom of the two quartz tubes C which are inserted into the two thermoelectric sensors. At the beginning of a run the solute is placed outside the calorimeter on the platinum plate H. Then, the alumina tube D is slowly introduced into the quartz tube until the plate lies just above the open surface of the bath previously melted in the calorimeter. The plate is

fastened to the alumina tube by means of three platinum rods with a refractory cement E.

When the thermal equilibrium in the calorimeter is reached the plate is slid down into the bath by a translatory motion of the calorimeter equipment (A–D–E–F–H) induced by the electric motor B. The dissolution begins and goes on for about 30 min. The vertical motion of the plate inside the thermopile produces a thermal effect which must be separately measured during a "blank run". Such a run follows each dissolution. This thermal effect is minimised by an approptiate adjustment of the position of the plate towards the open surface of the bath.

Calorimeter calibration

Periodically the calorimeter is calibrated in the same configuration as that used during the dissolutions by producing known thermal effects in the bath, i.e. with the plate at its lowest position in the bath. The calibrating thermal effect is the enthalpic variation of pure platinum balls between two well known temperatures; the ambient temperature T_a which is determined at ±0.05 K before each drop into the bath through the alumina tube and the temperature of the calorimeter T_d. The proportional factor between the thermal energy actually produced and the recorded electric voltage depends principally on the temperature and the calorimetric configuration. The calibration effect is obtained by integration of the following heat capacity relation of the pure platinum (in J mol^{-1} K^{-1}) [19].

$$C_p = 24.5526 + 4.96594\,10^{-3}T + 1.20828\,10^{-7}T^2 + 15948T^{-2}$$

$$\Delta H = n\int_{T_a}^{T_d} C_p(T)\,\mathrm{d}T$$

where n is the amount of substance in the ball measured previously by weighing on an electronic precision balance. For each bath a group of drops is performed. After studying the discrepancy the mean value is calculated. The calibrating factor is 0.787 ± 0.025 mW μV^{-1}.

RESULTS AND DISCUSSION

Starting materials are pure nitrates (99.998% minimum for the solid solution samples and 99.8% minimum for the bath) from Aldrich for $CsNO_3$ and from Prolabo for KNO_3 and $NaNO_3$. The samples and the bath are prepared by weighing (Mettler AT250) in suitable proportions and by melting in a platinum crucible at a not too high temperature (generally at the highest 20 K over the liquidus temperature) in order to prevent thermal decomposition of the nitrates. The homogeneity of the baths' composition is assumed by setting them apart a great amount of the ternary eutectic that has been previously homogenised in the liquid state.

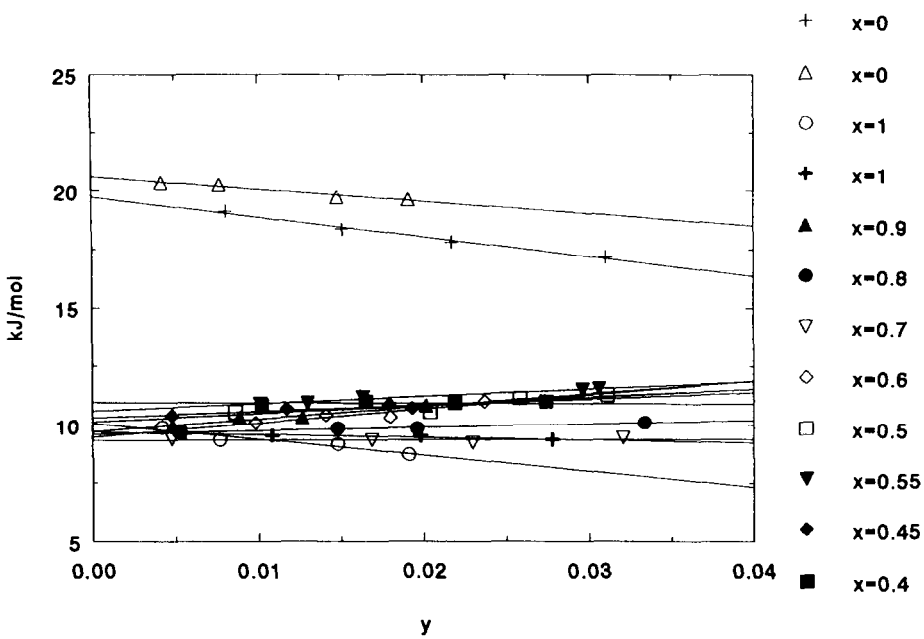

Fig. 2. Dissolution enthalpies of the solid solutions $(K_x, Na_{1-x})NO_3$ at 474 K in the (Na, Cs, K)NO_3 ternary eutectic. y Represents the molar fraction of the solute in the bath.

The previous thermal analysis experiments have shown that the kinetics of the α–β transformation in the solid solution are relatively fast. In fact they occur completely for a heating rate of almost any kelvin per minute, so during the thermal stabilisation of the calorimeter (which lasts for at least half an hour) the samples initially in the α state are completely transformed into the β structure.

As mentioned above, for each selected solid solution composition many samples are dissolved in the same bath so that the maximum of the solute molar concentration y in each bath is less than 0.035. The plot of the partial dissolution enthalpies versus the solute concentration y in the bath is always a straight line as shown in Fig. 2. The extrapolations to zero concentration in the bath give the partial dissolution enthalpies at infinite dilution which are reported in Table 1 with the corresponding standard deviation σ given by $[\sum (y - y_i)^2/(n-2)]^{1/2}$, n being the number of data points for each composition.

From these data, the mixing enthalpies in the solid solution referring to the pure nitrates in the same structure β are obtained with the equation

$$\Delta_m H = x\Delta_s H^{\infty}_{KNO_3} + (1-x)\Delta_s H^{\infty}_{NaNO_3} - \Delta_s H^{\infty}_{(K_x, Na_{1-x})NO_3} - (1-x)\Delta_{tr} H_{NaNO_3}$$

deduced from the eqs. (4) and (5). The results are reported in Table 2 and in Fig. 3. Before the solid solution dissolutions and in order to estimate the inaccuracy due to the compositional inhomogeneity of the baths, two series

TABLE 1

Partial dissolution enthalpies at infinite dilution of the solid solutions $(K_x,Na_{1-x})NO_3$ at 474 K

x	ΔH^{∞}_{diss} in J mol^{-1}	σ in J mol^{-1}
0.00	20083	118 (α phase)
0.40	10774, 10703	88
0.45	10021	213
0.50	10314, 10355, 10529	115
0.55	10263	370
0.60	9284, 9360, 9623, 9824	330
0.70	9330, 9958	92
0.80	9623	323
0.85	10238, 10167	59
0.90	9832	163
1.00	10042	116

of five runs were performed by using four different baths each sampling the single ternary mixture. In both cases, the reproducibility of the distinct extrapolations at infinite dilution is ±420 J. There is hence a major effect on the extrapolated data relative to the solid solution concentrations. For evaluation of the mixing enthalpies, this has been taken into account when determining a mean value of the dissolution enthalpies at infinite dilution for the pure nitrates.

The solid solution presents a positive deviation from ideality and a shift of the maximum to the sodium rich concentration range.

Both pure nitrate structures can be described as very close rhombohedral unit cells; $a = 4.15$ Å, axial angle 75°31′ for sodium nitrate and $a = 4.49$ Å, axial angle 73°50′ for potassium nitrate [20]. In the following we consider that the volume difference between the two cations induces this deviation from ideality and the shift of the maximum of mixing enthalpy. In the Van Laar model for a binary mixture AB [21], the mixing enthalpy can be

TABLE 2

Mixing enthalpies in the solid solutions $(K_x,Na_{1-x})NO_3$ referred to the pure nitrates in the same structure β at 474 K

x	$\Delta_m H$ in J mol^{-1}	x	$\Delta_m H$ in J mol^{-1}
0.00	0	0.70	2913, 2582
0.40	3271, 3342	0.80	1753
0.45	3690	0.85	1506
0.50	3064, 3023, 2849	0.90	877
0.55	3098	1.00	0
0.60	3426, 3351, 3088, 2887		

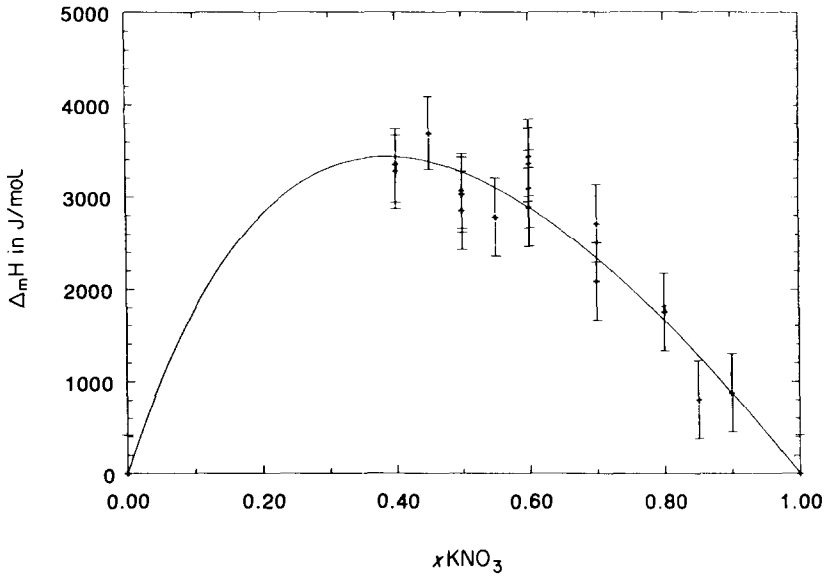

Fig. 3. Mixing enthalpy in the solid solution $(K_x,Na_{1-x})NO_3$ at 474 K. The stability range at this temperature is $0.38 < x < 1$. The curve represents the fit of the data with a Van Laar equation and $\mu = 0.40$.

written as a function of the partial mixing enthalpy at infinite dilution ΔH_A^∞, the concentration x_B and the volume ratio of the species ($\mu = V_A/V_B$). Thus, the ratio of the enthalpies at infinite dilution equals the volume ratio μ.

$$\Delta_m H = \Delta H_A^\infty \frac{x_B(1-x_B)}{x_B + (1-x_B)\mu}$$

$$\frac{\Delta H_A^\infty}{\Delta H_B^\infty} = \frac{V_A}{V_B} = \mu$$

In the literature the ionic radii are given as $r_K = 1.33$ Å and $r_{Na} = 0.98$ Å [20]. The ratio μ then equals 0.40. The fit of the experimental results with that expression is shown in Fig. 3. The enthalpies at infinite dilution can then be deduced; for sodium nitrate 9140 J mol^{-1} and for potassium nitrate 22850 J mol^{-1}.

In order to stabilise this phase at the high concentrations an excess entropy term is necessary. The maximum ideal entropy at $x = 0.5$ is about 5.76 J mol^{-1} K^{-1}; at 474 K the contribution to the free energy will be $-TS = -2.73$ kJ mol^{-1}. This contribution is insufficient. If we suppose that the probability of finding a cation A^+ on a cationic site is not x_A but Φ_A, the volume fraction

$$\Phi_A = \frac{x_A V_A}{x_A V_A + x_B V_B}$$

the maximum of an another ideal entropy can be calculated at 6.6 J mol^{-1} K^{-1} for a concentration close to 0.5 the contribution to the free energy of which is $-TS = -3.13$ kJ mol^{-1} at the same temperature. The stabilisation is then increased but an excess entropy seems to be necessary to make the free energy negative. Some preliminary attempts for coherency between the phase diagram and the thermodynamic properties in this system show that the maximum of the excess entropy which is necessary is about 5.3 J mol^{-1} K^{-1}. Such an excess entropy may be found in excess vibrational, or more probably, rotational disorder of the nitrate anions in the solid solution. From this point of view some structural studies and free enthalpy measurements of the solid solution would be of great interest.

The drawing of the $NaNO_3$–KNO_3 phase diagram is apparently simple; it does not present for instance any stoichiometric or non-stoichiometric compounds which make the reading difficult. The particularities of such a diagram are more subtle. First, despite that the second order phase transitions α–β in the pure nitrates are well known, the incidence of these transformations on the low temperature phase diagram is not clear. The existence of the subliquidus continuous solid solution is still ensured. Second, the presence of a liquidus with a minimum shows that the stabilities of the liquid and the subsolidus continuous solid solutions are very close. These measurements show that entropy plays an important role in the stabilisation of this subsolidus solid solution.

REFERENCES

1 H. Zamali and M. Jemal, XVI^{ème} Journées de l'Association Française de Calorimétrie et d'Analyse Thermique, Montpellier, France, 1985, pp. 298–304.
2 H. Zamali and M. Jemal, Diagrammes de phases binaires KNO_3–$NaNO_3$ et $CsNO_3$–KNO_3, to be published.
3 T. Jriri, personal communication, 1991.
4 G.G. Diogenov and I.F. Sarapulova, in E.M. Levin, C.R. Robbins, H.F. McMurdie and M.K. Reser (Eds.), Phase Diagrams for Ceramists, Am. Ceram. Soc., Columbus, Ohio, USA, 1969, p. 235, Fig. 2825.
5 D.J. Rogers and G.J. Janz, J. Chem. Eng. Data, 27 (1982) 424–428.
6 D.I. Marchidan and C.R. Telea, Rev. Roum. de Chim., 13 (1968) 1291–1295.
7 O.J. Kleppa, J. Chem. Phys., 64(12) (1960) 1937–1940.
8 T. Förland, in B.R. Sundheim (Ed.), Fused Salts, McGraw Hill, New York, 1964; J. Am. Chem. Soc., 79 (1957) 1849–1851.
9 B.F. Powers, J.L. Katz and O.J. Kleppa, J. Chem. Phys., 66(12) (1962) 103–105.
10 O.J. Kleppa and L.S. Hersh, J. Chem. Phys., 34(2) (1961) 351–358.
11 J. Quinard, E.K. Omari, Alaoui, R. Martin and C. Boyer, J. Chim. Phys., 80(11–12) (1983) 771–776.
12 R. Vilcu, F. Irinei and E. Tatu, Rev. Roum. Chim., 21(4) (1976) 491–494.
13 M. Blander, Molten Salt Chemistry, Wiley, New York, 1964.
14 C.M. Kramer and C.J. Wilson, Thermochim. Acta, 42 (1980) 253–264.
15 N. Mossarello, Thesis, University Aix-Marseille I, France, 1986.
16 Y. Dessreault, J. Sangster and A.D. Pelton, J. Chim. Phys., 87 (1990) 407–453.

17 E. Calvet and H. Prat, Recent Progress in Microcalorimetry, Pergamon Press, Oxford, 1963.
18 E. Calvet and H. Prat, Microcalorimétrie: Applications physico-chimiques et biologiques, Masson, Paris, 1956.
19 A.T. Dinsdale, N.P.L. Report (A) 195 of the Division of Materials Applications in the National Physical Laboratory, 1989, Teddington, UK, pp. 189–192.
20 D.M. Newns and L.A.K. Staveley, Chem. Rev., 66 (1966) 267–278.
21 M. Van Laar, Z. Phys. Chem., 72 (1910) 723.